Cardiomyocyte Dysfunction in Sucrose-Fed Rats Is Associated With Insulin Resistance

Kaushik Dutta, Deborah A. Podolin, Michael B. Davidson, and Amy J. Davidoff

Diabetes is associated with impaired cardiac dysfunction in both humans and animals. Specific phenotypic changes—prolonged action potentials, slowed cytosolic Ca^{2+} clearing, and slowed relaxation—that contribute to this whole heart dysfunction occur in isolated ventricular myocytes. The present study was designed to determine whether cardiomyocyte abnormalities occur early in the development of type 2 diabetes (in this case, insulin resistance) and whether an insulin-sensitizing drug (metformin) is cardioprotective. In the study, high-sucrose feeding was used to induce whole-body insulin resistance. Wistar rats were maintained for 7–10 weeks on a starch (ST) diet, sucrose (SU) diet, or diet supplemented with metformin (SU + MET). Whole-body insulin resistance was measured in SU and SU + MET rats by performing euglycemic-hyperinsulinemic clamps. Mechanical properties of isolated ventricular myocytes were measured by high-speed video edge detection, and $[Ca^{2+}]_i$ transients were evaluated with Fura-2 AM. Untreated SU rats were insulin-resistant (glucose infusion rate [GIR] = 14.5 ± 1.1 mg · kg^{-1} · min^{-1}); metformin treatment in SU + MET rats prevented this metabolic abnormality (GIR = 20.0 ± 2.2 mg · kg^{-1} · min^{-1}). Indexes of myocyte shortening and relengthening were significantly longer in SU rats (area under the relaxation phase [A_R/peak] = 103 ± 3 msec) when compared to ST and SU + MET rats (A_R/peak = 73 ± 2 and 80 ± 1 msec, respectively). The rate of intracellular Ca^{2+} decay and the integral of the Ca^{2+} transient through the entire contractile cycle were significantly longer in myocytes from SU than from ST rats (Ca^{2+} signal normalized to peak amplitude = 152 ± 8 vs. 135 ± 5 msec, respectively). Collectively, our data showed the presence of cardiomyocyte abnormalities in an insulin-resistant stage that precedes frank type 2 diabetes. Furthermore, metformin prevented the development of sucrose-induced insulin resistance and the consequent cardiomyocyte dysfunction. *Diabetes* 50:1186–1192, 2001

From the College of Osteopathic Medicine, University of New England, Biddeford, Maine.

Address correspondence and reprint requests to Amy J. Davidoff, PhD, University of New England, 11 Hills Beach Rd., Biddeford, ME 04005. E-mail: adavidoff@mailbox.une.edu.

Received for publication 24 August 2000 and accepted in revised form 23 January 2001.

A_C, area under the contractile phase; A_R, area under the relaxation phase; $Area_{Ca2+}$, Ca^{2+} signal normalized to peak amplitude; 2-DG, 2-deoxy-D-[1-^{14}C] glucose; GIR, glucose infusion rate; KHBB, Krebs-Henseleit bicarbonate buffer; PS, peak fractional shortening; PT, peak twitch amplitude; ST, high-starch; SU, high-sucrose; SU + MET, SU diet supplemented with metformin; TPT, time to peak twitch amplitude; TR, time of relengthening from peak twitch amplitude.

Cadiovascular disease is a leading cause of morbidity and mortality in type 2 diabetes. Abnormal ventricular systole and diastole are reported in both type 1 and 2 diabetic patients presenting without macrovascular disease or hypertension, which provides indirect evidence that there is diabetic cardiomyopathy in humans (1,2). Furthermore, in clinical studies, detectable cardiac dysfunction has been reported to occur as early as the glucose intolerance phase—that is, hyperinsulinemia and hyperglycemia—that follows insulin resistance (3). Diastolic abnormalities (including prolonged relaxation) precede impaired systolic activity (4).

More direct evidence of diabetic cardiomyopathy has come from various animal models of diabetes (5–7). The cellular mechanisms of diabetic cardiomyopathy in models of type 1 diabetes are well characterized, but relatively little is known about the pathogenesis of cardiomyopathy in type 2 diabetes (8,9). In type 1 diabetes, abnormal cardiomyocyte excitation-contraction coupling includes prolonged action potentials, slowed cytosolic Ca^{2+} clearing, depressed peak fractional shortening, and prolonged contraction and relaxation (10–12). Remarkably, these cellular changes occur within days after the onset of diabetes and provide insight into the pathogenesis of cardiomyopathy (12–14). Regardless of whether cellular changes arise from microvascular complications (e.g., sustained or transient ischemia), the abnormalities persist in isolated cardiomyocytes (10,12,13,15).

Type 2 diabetes is clinically more prevalent than type 1, but understanding the pathogenesis of cardiomyopathy is complicated by numerous comorbidities in both humans and animals (e.g., hypertension, obesity, hyperinsulinemia, hyperglycemia, and dyslipidemia). To this end, we chose an animal model that presents with relatively minor metabolic abnormalities, consistent with prediabetic insulin resistance in humans (16–18), and that mimics early stages of type 2 diabetes. High-sucrose feeding has been used to induce whole-body insulin resistance, and the time course of the metabolic changes are highly reproducible (16,18). For example, sucrose-fed rats become hypertriglyceridemic between weeks 1 and 2 and exhibit whole-body insulin resistance and hyperinsulinemia after 2 weeks (16). In this particular model (unlike many genetic models of type 2 diabetes or fructose feeding), sucrose feeding does not produce obesity or hypertension, therefore avoiding hemodynamic changes that can independently alter cardiac physiology.

Metformin, a biguanide, is an antidiabetic agent that is

Downloaded from http://diabetesjournals.org/diabetes/article-pdf/50/5/1186/367163/1186.pdf by guest on 06 December 2024

currently being used in clinical therapy to control and treat metabolic changes associated with type 2 diabetes. Metformin is believed to exert its antihyperglycemic action by potentiating insulin action and reducing insulin resistance, but the precise mechanisms by which this occurs are still unclear. Biguanides have been shown to lower blood pressure, blood glucose, plasma triglycerides, and hepatic gluconeogenesis in type 2 diabetic patients (19). Metformin treatment also lowers blood pressure and plasma insulin in a hyperinsulinemic animal model (20) and attenuates the development of impaired cardiac performance in type 1 diabetic rats (21).

The present study was designed to determine whether a cardiomyocyte dysfunction exists in diet-induced insulin-resistant rats and whether the development of these cellular dysfunctions are prevented by metformin treatment. Our data support the view that a diabetic-like cardiomyopathy is apparent at very early stages of type 2 diabetes and is associated with insulin resistance.

RESEARCH DESIGN AND METHODS

Animals. Wistar rats weighing 120–140 g (Charles River Breeding Lab, Wilmington, MA) were housed individually and put on either a high-starch (ST) diet (68% of total energy from cornstarch) or high-sucrose (SU) diet (68% of total energy from sucrose) formulated by Research Diets (New Brunswick, NJ). The diets included all necessary constituents for growth (17) and contained 68% carbohydrate, 20% protein, and 12% fat. A separate cohort of rats was fed an SU diet (as above) or an SU diet supplemented with metformin in drinking water (SU + MET). Metformin was dissolved in the drinking water, and body weight and water volume consumption were monitored to ensure that ~500 mg · kg^{-1} · day^{-1} were administered (21). The presence of metformin in the drinking water did not alter the volume of water consumed. After 7–10 weeks on diet and treatment, rats were either killed for ventricular myocyte isolation or prepared for euglycemic-hyperinsulinemic clamps for the assessment of whole-body insulin resistance (see below).

Ventricular myocyte isolation. Animals were anesthetized by injecting a 1:7 ketamine/xylazine mixture (184 mg/kg i.p.). Single ventricular myocytes were isolated by methods previously described (12). In brief, hearts were perfused with a Krebs-Henseleit bicarbonate buffer (KHBB), containing (in mmol/l) 118 NaCl, 4.7 KCl, 1.25 $CaCl_2$, 1.2 $MgSO_4$, 1.2 KH_2PO_4, 11.1 glucose, 10 HEPES, and 25 $NaHCO_3$, equilibrated with 95% O_2–5% CO_2, with a pH of 7.4 at 37°C. The KHBB was then replaced with a Ca^{2+}-free KHBB for 2–3 min until the spontaneous contractions ceased. The perfusate was then switched to a Ca^{2+}-free KHBB containing 169 U/ml collagenase type 2 (Worthington Biochemical, Freehold, NJ) and 0.1 mg/ml hyaluronidase (Sigma, St. Louis, MO) for 26 min. After perfusion, the ventricles were separated from the great vessels and atria, minced, and gently triturated for 3–5 min in the above enzyme solution supplemented with 0.02 mg/ml trypsin (Sigma). The cells were filtered through a nylon mesh (300 μm) and resuspended in a Ca^{2+}-free modified Tyrode's buffer containing (in mmol/l) 131 NaCl, 4 KCl, 1 $MgCl_2$, 10 glucose, and 10 HEPES as well as 2% bovine serum albumin, with a pH of 7.4 at 37°C. A pellet of myocytes was separated from the suspension by centrifugation (60*g* for 60 s). Myocytes were then resuspended in a new aliquot of buffer to remove remnant enzyme and to increase extracellular Ca^{2+} incrementally. This washing process was repeated five times, resulting in a final concentration of 1 mmol/l Ca^{2+}. Myocytes were resuspended in Ca^{2+} containing Tyrode's buffer without albumin, plated onto laminin-coated (10 μg/ml; Collaborative Biochemical, Bedford, MA) glass coverslips, and allowed to attach for 20–30 min at 37°C. Within this time frame, viable rod-shaped myocytes attached to the laminin substrate; the dead myocytes were then washed off. Myocytes (attached to coverslips) were stored in Tyrode's buffer at 37°C in a 100% humidity and 5% CO_2 incubator until used. Mechanical properties and Ca^{2+} transients were recorded in myocytes within 6 h after isolation. We have previously found that fura-2 loading slows myocyte mechanics; therefore, we recorded myocyte twitches and Ca^{2+} transients in separate groups of cells.

Measurement of myocyte shortening/relengthening. Mechanical properties of isolated ventricular myocytes were assessed by video-edge detection (IonOptix, Milton, MA). The coverslips with cells attached were placed in a perfusion bath (1 ml vol) mounted on the stage of an inverted microscope. The microscope was housed in a large chamber with the ambient air temperature maintained at 32 ± 1°C. The cells were superfused at a flow rate of ~2 ml/min with Tyrode's buffer containing 1 mmol/l Ca^{2+}. Myocytes were field-stimulated to contract by a 3 ms square wave pulse through a bipolar platinum electrode, at a stimulus frequency of 0.5 Hz. An image of myocyte motion was detected by a charged coupled device camera; the longitudinal edges were tracked and the pixel displacements of left and right edges were calibrated (in microns) and plotted over time (IonOptix). The video sweep speed was set at 240 Hz to yield high-fidelity sampling. For each myocyte, ~10 steady-state twitches were averaged and further analyzed offline with Clampfit (Axon Instruments, Foster City, CA). The indexes used to evaluate myocyte mechanics are described in RESULTS (see Fig. 1*A*).

Measurement of intracellular Ca^{2+}. In subsets of myocytes isolated from rats described above, intracellular Ca^{2+} transients were recorded by a dual-excitation fluorescence photomultiplier system (IonOptix), as previously described (12). Myocytes were loaded with 0.5 μmol/l Fura-2 AM (Molecular Probes, Eugene, OR) suspended in physiological buffer containing 0.2% albumin for ~20 min at room temperature. Myocytes were placed on an inverted microscope equipped with a heated (32 ± 1°C) and light-tight chamber, imaged through a 20× water emersion objective, and field stimulated to contract at a frequency of 0.5 Hz. Cells were exposed to light passed through a 360- or 380-nm filter (band width 15 nm). Fluorescence emissions were detected at 480–520 nm by a photomultiplier tube after illuminating cells at 360 nm for 0.5 s then at 380 nm for the duration of the recording protocol (1 kHz). The 360-nm excitation scan was repeated at the end of each transient, and an interpolated signal was determined and used to calculate the ratio with the 380-nm emission. The decay of the Fura signal from peak was described by a single exponential equation, and the rate of cytosolic Ca^{2+} clearing was determined by the time constant (τ) of the equation. We also determined the total area under each Ca^{2+} transient normalized to the peak signal to account for the time course of the overall contractile cycle. Curve fitting and signal integrations were measured with Clampfit (Axon Instruments).

Euglycemic-hyperinsulinemic clamps. Whole-animal insulin resistance was evaluated in a subset of sucrose-fed rats (16,18). After the 7- to 10-week dietary period, euglycemic-hyperinsulinemic clamps were performed. In preparation for the clamps, the left carotid artery and right jugular vein were cannulated. Briefly, rats were anesthetized with the same ketamine/xylazine mixture as described above (delivered intraperitoneally) and cannulas (PE 50) were inserted into both the carotid artery (advanced up to the aortic arch) and the jugular vein (advanced up to the vena cava). The cannulas were then sutured to the respective vessel and exteriorized through the back of the neck. Animals were allowed at least 3 days to recover from surgery and were required to have reached 93% of presurgery body weight to be studied.

On the day of the experiment, extensions were added to cannulas for ease of sampling; the rats were then allowed to rest for 20 min. A baseline blood sample (for preclamp plasma glucose and insulin concentrations) was taken. The clamp began with a primed, continuous infusion of insulin (4 mU · kg^{-1} · min^{-1}). A variable glucose infusion (10% dextrose) was used to maintain plasma glucose at preclamp values. Arterial blood was sampled every 5 min, and the glucose infusion rate was adjusted accordingly to maintain euglycemia (110–120 mg/dl). After ~45 min, a bolus injection of 2-deoxy-D-[1-^{14}C]glucose (2-DG) was administered via the carotid cannula when plasma glucose levels were at a steady state. Blood samples were taken at 2.5, 5, 10, 15, 20, 30, 37.5, and 45 min for 2-DG levels and during the final blood sample for circulating insulin concentrations. Blood samples were collected with a heparinized syringe and immediately centrifuged; the plasma was frozen at –70°C for later analyses. Plasma glucose levels were determined by the glucose oxidase method (16,18) using a Beckman glucose analyzer (Fullerton, CA). Plasma insulin was measured by radioimmunoassay (Linco Research, St. Louis, MO).

Statistical analyses. All data were statistically evaluated using an unpaired *t* test or its nonparametric equivalent (Wilcoxon's rank-sum test) if sample sizes were <20. Each index was assessed separately (SYSTAT, Chicago, IL); statistical significance was considered at $P < 0.05$.

RESULTS

Sucrose feeding induces whole-body insulin resistance and is prevented by metformin. Animals were matched according to weight at the beginning of the study and fed so that the body weight of the ST and SU groups remained similar. After 7–10 weeks on diet, there were no significant differences in body weight attributable to diet (Table 1). Weight-matched feeding is an important component of this study because obesity in itself is associated with insulin resistance and cardiac dysfunction. Another important characteristic of this model is that sucrose

Downloaded from http://diabetesjournals.org/diabetes/article-pdf/50/5/1186/367163/1186.pdf by guest on 06 December 2024

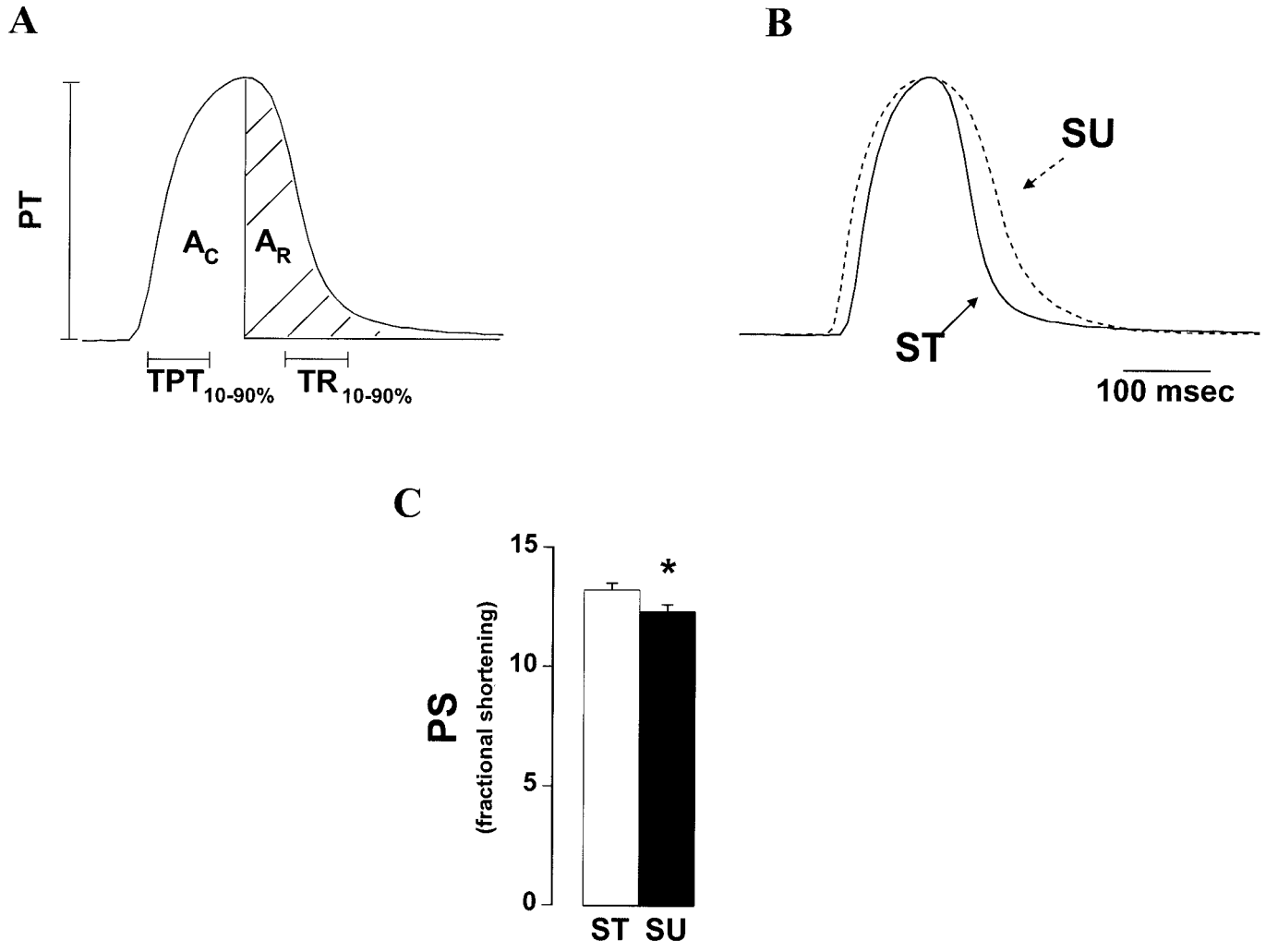

FIG. 1. ***A*: Indexes used to evaluate shortening and relengthening of myocyte twitch.** ***B:*** **Representative twitches of ventricular myocytes isolated from ST and SU rats. Twitches were chosen that best represent the means of shortening and relengthening for each group. PTs were normalized to each other to illustrate the time course of each twitch.** ***C*: PS for ST and SU rats. PS is PT expressed as the percentage of resting cell length. Data represent means ± SE from 106–181 cells per diet (isolated from 6–8 hearts per diet). *$P < 0.05$ between diets.**

feeding induces hyperinsulinemia while euglycemia is maintained (16,17). Initially, blood samples were taken in anesthetized rats just before excising the heart. We found that the ketamine/xylazine preparation significantly suppressed insulin secretion in all groups. Therefore, we cannulated subsequent rats and collected blood from the carotid artery in unanesthetized and quiescent rats. As previously reported, SU rats were euglycemic and hyperinsulinemic relative to the ST rats (Table 1).

To determine whether metformin treatment would effectively prevent insulin resistance, euglycemic-hyperglycemic clamps were performed on a subset of SU rats and SU + MET rats. Before the clamp, plasma glucose levels were similar between groups (Table 2), and plasma insulin levels were significantly elevated in the SU compared with the SU + MET rats. The glucose infusion rate (GIR) was significantly lower in the SU rats compared to the SU + MET rats, despite similar steady-state plasma glucose and insulin levels (Table 2). These data confirmed that the sucrose-fed rats were insulin-resistant, and demonstrated that metformin prevented the development of insulin resistance.

TABLE 1
Body weight, serum glucose, and insulin values of rats fed either a high-starch or sucrose diet

Group	Body weight (g)	Glucose (mg/dl)	Insulin (μU/ml)
Starch	544 ± 18	125 ± 7	94 ± 10
Sucrose	525 ± 19	127 ± 4	128 ± 9*

Data are means ± SE, n = 8–10 animals/diet. Rats were fasted for ~6–8 h before serum collection. *$P < 0.05$ vs. starch group.

TABLE 2
Serum glucose and insulin values of sucrose-fed rats treated with or without metformin, before and during euglycemic-hyperinsulinemic clamps

Group	Fasting glucose (mg/dl)	Fasting insulin (μU/ml)	Clamp glucose (mg/dl)	Clamp insulin (μU/ml)	GIR (mg/kg/min)
Sucrose	135 ± 2	92 ± 8	123 ± 8	247 ± 43	14.5 ± 1.1
Sucrose + metformin	132 ± 5	58 ± 2*	117 ± 6	244 ± 34	20.0 ± 2.2*

Data are means ± SE; n = 4 animals/group. For fasting values, rats were fasted ~6–8 h before serum collection. *$P < 0.05$ vs. sucrose group.

Downloaded from http://diabetesjournals.org/diabetes/article-pdf/50/5/1186/367163/1186.pdf by guest on 06 December 2024

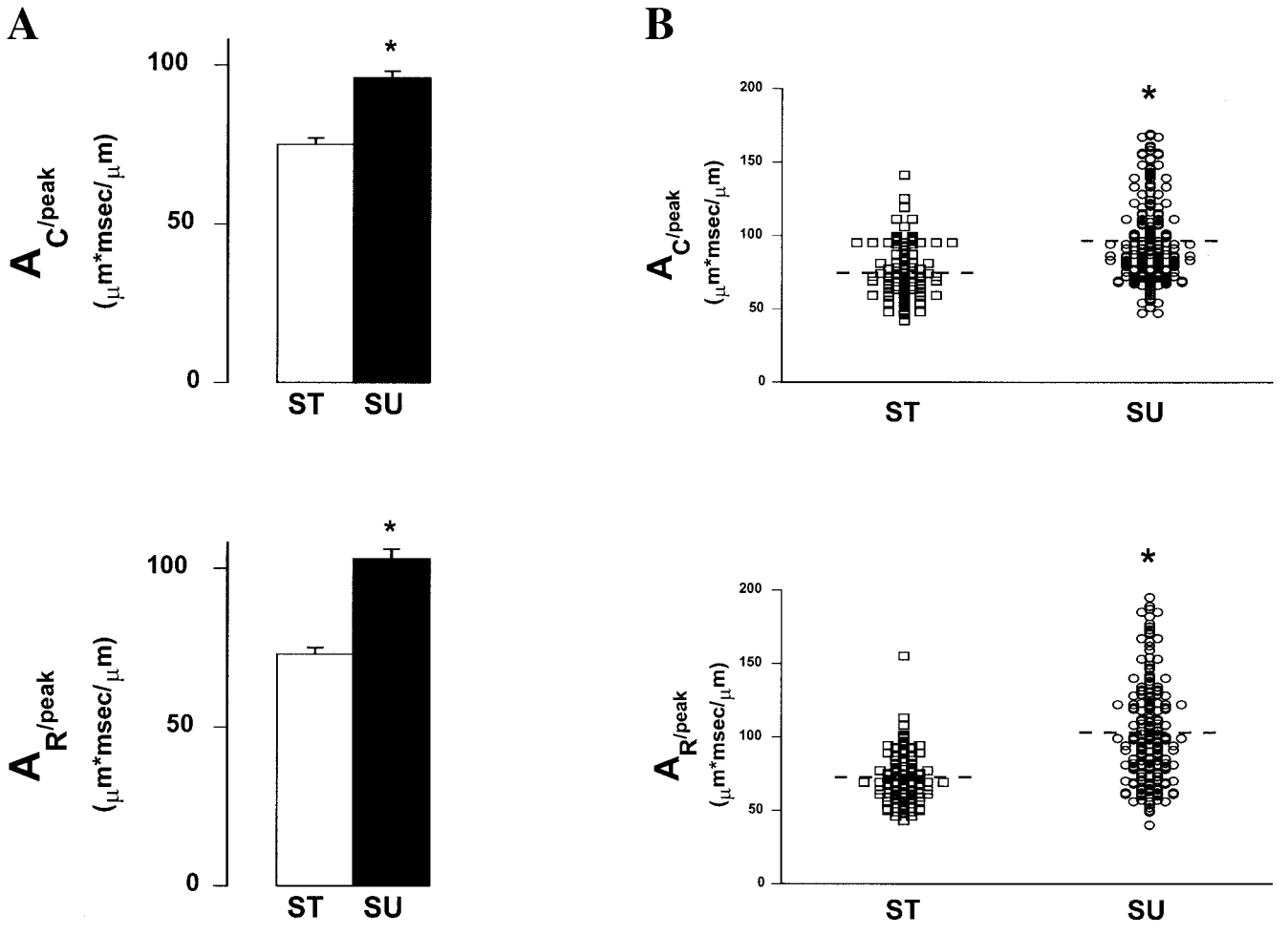

FIG. 2. *A*: **Contraction (A_C/peak) and relaxation (A_R/peak) properties of myocytes from ST and SU rats. Integrated indexes (A_C and A_R) were normalized to PT.** *B*: **Scatter plots are the individual data points used to generate the summary data. They depict the distribution of these data (dashed lines represent mean values for each index). Data represent either means ± SE or individual data points from 106–181 cells per diet (isolated from 6–8 hearts per diet). *$P < 0.05$ between diets.**

Insulin resistance induces myocyte mechanical dysfunction. The mechanical properties of isolated ventricular myocytes were recorded to determine whether insulin resistance leads to abnormal cardiomyocyte function. Only rod-shaped myocytes with clear edges were selected for recording mechanical properties and Ca^{2+} transients. The indexes of shortening and relengthening (Fig. 1*A*) were recorded at a slow stimulus frequency (0.5 Hz), using only cells that exhibited steady-state twitches. Sucrose feeding did not affect the longitudinal length of myocytes (130 ± 2 [ST group] vs. 125 ± 2 μm [SU group]; n = 106–181 cells per diet).

Representative twitches of myocytes from ST and SU rats are presented in Fig. 1*B*. The traces were normalized to the peak twitch amplitude (PT) to better illustrate the effect of sucrose feeding on shortening and relengthening phases. Peak fractional cell shortening (PS) (the PT normalized to resting cell length) was significantly depressed in ventricular myocytes isolated from the insulin-resistant SU rats when compared with the normal ST rats (Fig. 1*C*).

Two indexes were used to assess the time course of the contractile phase: time from 10% above baseline to 90% peak twitch (TPT) and area under the rising phase of the curve (A_C) (Fig. 1*A*). The A_C index was expressed relative to the PT to account for its effect on area (A_C/peak). A slower TPT was evident in SU myocytes (71 ± 1 msec; n = 181) compared to ST myocytes (55 ± 1 msec; n = 106). Similarly, sucrose feeding increased the A_C/peak (Fig. 2*A*), indicating that insulin resistance is associated with slowed myocyte contraction. Myocyte relaxation was evaluated by time from 10% below peak twitch to 90% relengthening (TR) and the area under the falling phase of the curve (A_R) (Fig. 1*A*) normalized to the PT (A_R/peak). TR was longer in the SU myocytes (105 ± 4 msec; n = 181) than in the ST myocytes (83 ± 3 msec; n = 106). Sucrose feeding increased the A_R/peak (Fig. 2*A*), indicating that cardiomyocyte relaxation was impaired in the insulin-resistant rats. Figure 2*B* illustrates individual data points for the A_C/peak and A_R/peak and shows that there was a heterogeneous effect on myocyte mechanics. Insulin resistance did not affect each myocyte uniformly, so that a portion of the myocytes from SU rats had normal contractile properties. However, the cumulative effects of sucrose feeding resulted in a population of myocytes with impaired contraction and relaxation.

Abnormal Ca^{2+} transients contribute to myocyte dysfunction. We evaluated the time course of cytosolic Ca^{2+} clearing to determine whether slowed transient decay was associated with abnormal relaxation in myocytes from insulin-resistant rats. We used the Ca^{2+}-sensitive and

Downloaded from http://diabetesjournals.org/diabetes/article-pdf/50/5/1186/367163/1186.pdf by guest on 06 December 2024

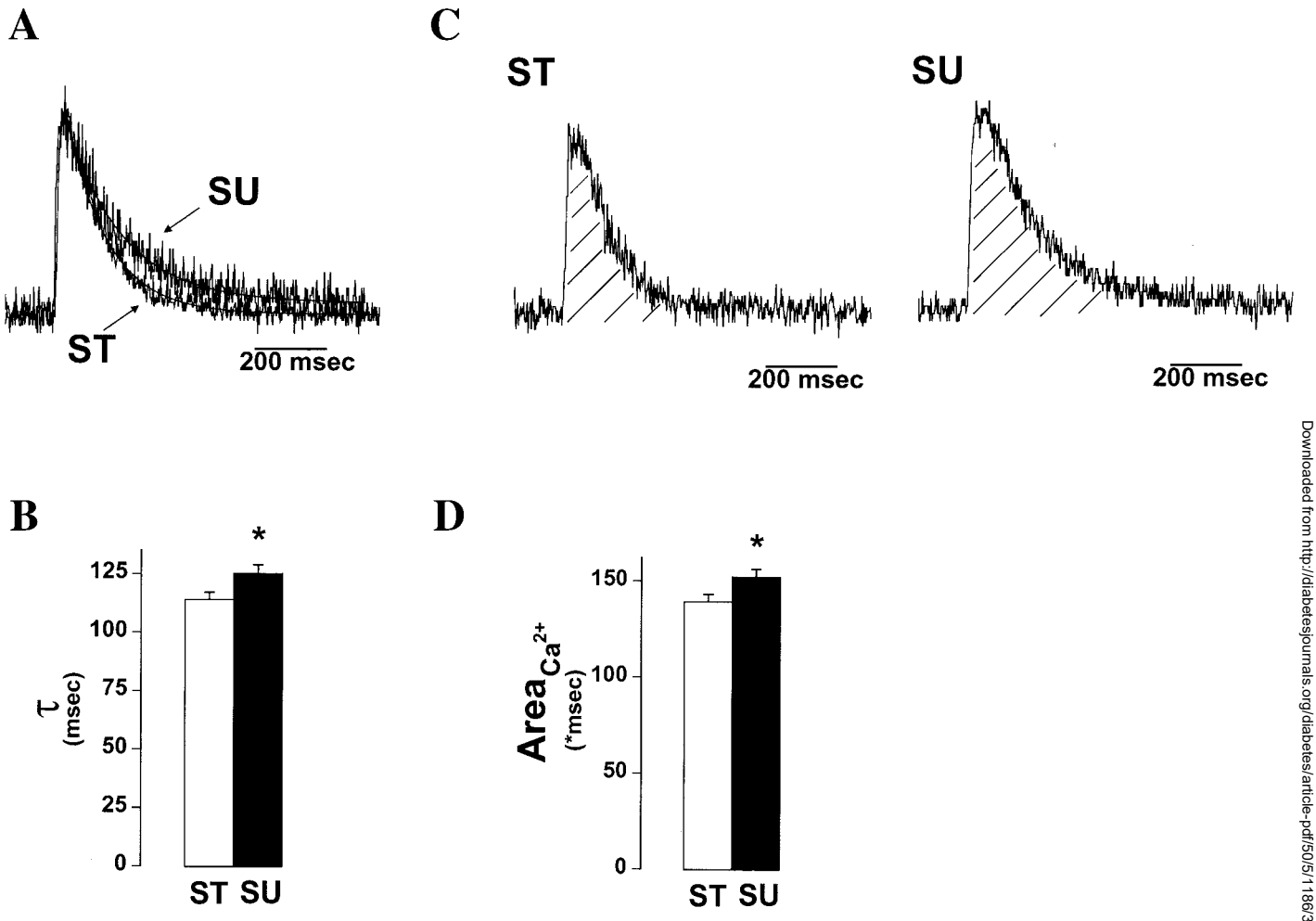

FIG. 3. Ca^{2+} transients recorded from fura-2–loaded ventricular myocytes isolated from ST and SU rats. *A*: Ca^{2+} transient decay was evaluated by curve fitting the falling phase of the signal with a single exponential equation and expressing the time constant τ. The superimposed lines illustrate the calculated fits. *B*: Bar graph of summary data for the time constant τ. *C*: Integration of Ca^{2+} signals ([hatch lines]) for ST and SU rats. *D*: Bar graph of summary data for the integrated Ca^{2+} transients normalized to peak ($Area_{Ca2+}$). Data represent means ± SE from 85–89 cells per diet (isolated from 6–7 hearts per diet). *$P < 0.05$ between diets.

membrane-permeant form of Fura-2 to measure the time course of intracellular Ca^{2+} transients in isolated myocytes. A single exponential equation was used to describe the decay of the 360/380 fluorescence signal as an index for the time course of cytosolic Ca^{2+} clearing (Fig. 3*A*). The time constant (τ) for the decay of free cytosolic Ca^{2+} was significantly longer in SU rats than in ST control rats, suggesting slowed cytoplasmic Ca^{2+} clearing (Fig. 3*B*). Ca^{2+} transients could only be adequately fit with a single exponential equation when the falling phase of the transient was considered; therefore, the τs only describe the time course of signal decay. To evaluate cytosolic Ca^{2+} dynamics over the course of the entire contraction-relaxation cycle, we integrated the Ca^{2+} signal and normalized it to the peak amplitude ($Area_{Ca2+}$) (Fig. 3*D*). $Area_{Ca2+}$ was larger in SU myocytes than in ST myocytes, indicating that cytosolic Ca^{2+} was prolonged in myocytes from insulin-resistant rats (Fig. 3*A*). There was a heterogeneous effect on cytosolic Ca^{2+} clearing in SU myocytes similar to that illustrated for the mechanical indexes in Fig. 2*B* (e.g., cytosolic Ca^{2+} clearing in some cells was normal).

Metformin protects against sucrose-induced prolonged contraction and relaxation. The question of whether whole-body insulin resistance leads to the development of cardiomyocyte dysfunction was addressed by evaluating myocyte mechanics in SU + MET rats. In this cohort, PS was unaffected by sucrose feeding or metformin (Fig. 4*A* when compared to ST control rats (Fig. 1*C*). This inconsistent effect on PS is not unlike that which has been reported in models of early-stage cardiomyopathy secondary to type 1 diabetes (22).

Indexes of contraction (A_C/peak) and relaxation (A_R/peak) were significantly smaller in SU + MET rats than in untreated SU rats. These indexes in the metformin-treated rats were the same as in the normal ST rats (compare Figs. 2*A* and 4*B* and *C*). When ST and SU + MET data were compared, a Bonferroni adjustment of α was used to account for multiple comparisons. Therefore, metformin prevented the development of the cardiomyocyte abnormalities in SU rats.

DISCUSSION

The principal findings of this investigation are that cardiomyocytes from insulin-resistant rats show mechanical defects that can be prevented by metformin treatment. We demonstrated for the first time that phenotypic changes occur during the insulin-resistant phase (representing a

Downloaded from http://diabetesjournals.org/diabetes/article-pdf/50/5/1186/367163/1186.pdf by guest on 06 December 2024

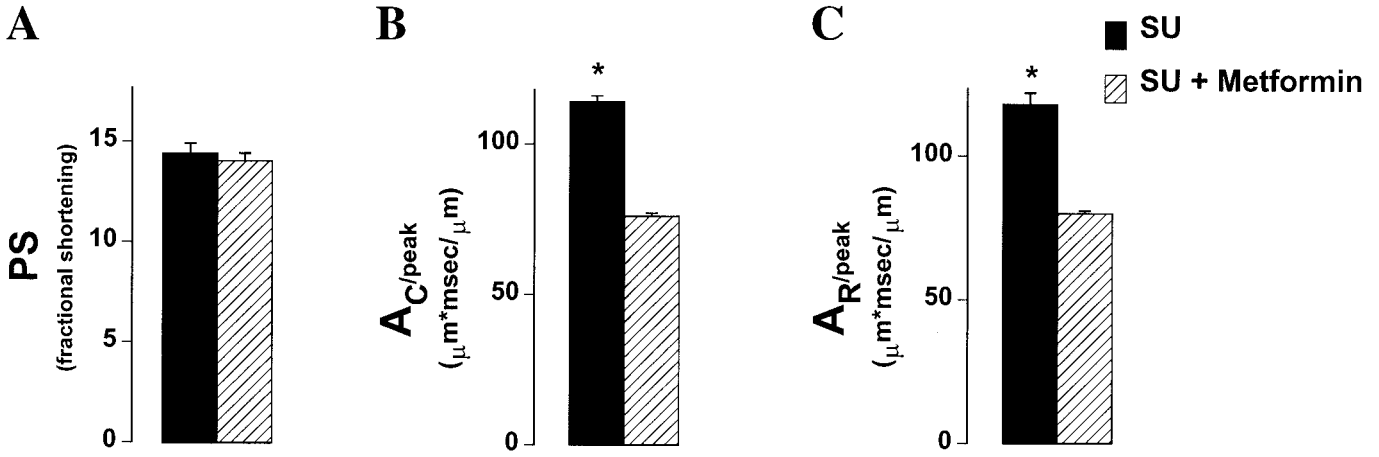

FIG. 4. Mechanical properties of myocytes from SU and SU + MET rats. PS (*A*) is PT expressed as the percentage of resting cell length. Myocyte contraction (A_C/peak) (*B*) and relaxation (A_R/peak) (*C*) are shown for SU and SU + MET rats. Data represent means ± SE from 49–97 cells per diet (isolated from 1–2 hearts per group) collected from a separate cohort of rats than those presented in Figs. 1–3. *$P < 0.05$ between treatments.

prediabetic state), and that these changes are similar to those seen in early stages of type 1 diabetes (12). The cardioprotective effects of metformin are associated with the prevention of insulin resistance, supporting the view that whole-body insulin resistance contributes to the pathogenesis of cardiomyocyte dysfunction in this model. The specific myocyte mechanical defects associated with sucrose feeding include slower rates of shortening and relengthening, slower cytosolic Ca^{2+} clearing, and depressed PS (albeit inconsistently) (Figs. 1*C* and 4*A*).

In the present study, sucrose feeding prolonged electrically stimulated Ca^{2+} transients in cardiomyocytes, and this prolongation most likely contributed to impaired myocyte relaxation. Myocardial contractile performance is dependent on intracellular Ca^{2+} concentration and its regulation. It remains to be determined whether expression and function of Ca^{2+}-regulating processes (e.g., sarcoplasmic reticulum Ca^{2+} uptake and Na^+/Ca^{2+} exchange) are depressed in myocytes from insulin-resistant animals, as shown in other models of type 1 and type 2 diabetes (23,24).

The variability of our myocyte mechanical data is intriguing because it clearly illustrates that there is a heterogeneous effect of insulin resistance on myocytes (illustrated by the individual data points for A_C/peak and A_R/peak in Fig. 2*B*). The summary data show that contraction and relaxation are prolonged in sucrose-fed rats (Fig. 2*A*). However, the population distribution figures show that a substantial number of myocytes in sucrose-fed rats are normal. We are confident that our mechanical data accurately reflect the population of isolated cells because measurements were made on >100 cells isolated from multiple rats for each diet. This heterogeneity among cells may explain why whole-heart dysfunction is not apparent in all models of type 2 diabetes. For example, in a streptozotocin-induced diabetic rat model of type 2 diabetes, whole-heart dysfunction developed after ~8 months, including depressed ventricular pressure generation, slower relaxation, and diminished cardiac output (5). Conversely, whole-heart function was normal under basal experimental conditions in fructose-fed animals (25) and in rat strains that are genetically predisposed to type 2 diabetes. Obvious changes in whole-heart function or isolated myocytes (26) do not become readily apparent except under severe conditions, such as ischemia, high extracellular Ca^{2+}, or rapid pacing (27,28). One possible explanation for these results is that there is a sufficient number of myocytes functioning normally that can compensate for the impaired cells.

Treatment with metformin was sufficient to prevent the fasting hyperinsulinemia found in untreated SU rats. SU + MET rats also required a higher rate of exogenous glucose infusion to maintain euglycemia during hyperinsulinemic clamps than did SU rats, indicating increased insulin responsiveness (Table 2). These data provide evidence that sucrose-induced whole-body insulin resistance is prevented by metformin. The mechanical indexes (A_C/peak and A_R/peak) for myocytes from SU + MET rats were identical to the normal ST rats (Figs. 2*A* and 4*B* and *C*). Therefore, by preventing the onset of whole-body insulin resistance, cardiomyopathy is also prevented. These data support the view that insulin resistance per se is sufficient to induce ventricular myocyte dysfunction.

Metformin therapy is used to minimize complications in type 2 diabetic patients. It is known to increase insulin sensitivity and reduce hepatic gluconeogenesis, but relatively little is known about its effects on the heart. Metformin treatment has been shown to reduce insulin resistance and normalize vascular responsiveness to norepinephrine in fructose-fed rats (20,29). Whether metformin has any direct effects on cardiac muscle has yet to be determined. However, we have recently shown that metformin prevents the development of glucose-induced cardiomyopathy in an in vitro model of type 1 diabetes, perhaps through tyrosine kinase-dependent signaling (30).

In summary, our data show that a diabetic-like cardiomyocyte dysfunction develops early on in the disease process, during the insulin-resistance phase, when metabolic disturbances are still relatively minor compared to end-stage diabetes. Furthermore, treatment with a clinically relevant pharmacological agent (metformin) prevents the phenotypic changes in ventricular myocytes associated with insulin resistance. This study provides a framework within which we can further characterize the underlying cellular consequences and determine the factors that contribute to the development of diabetic cardiomyopathy.

Downloaded from http://diabetesjournals.org/diabetes/article-pdf/50/5/1186/367163/1186.pdf by guest on 06 December 2024

ACKNOWLEDGMENTS

This research was supported by funding from National Institutes of Health Grant R01-HL-60303 (A.J.D.).

The authors are grateful for the technical assistance of Donna Lariviere.

REFERENCES

1. Zarich SW, Nesto RW: Diabetic cardiomyopathy. *Am Heart J* 118:1000–1012, 1989
2. Grundy SM, Benjamin IJ, Burke GL, Chait A, Eckel RH, Howard BV, Mitch W, Smith SC, Sowers JR: Diabetes and cardiovascular disease: a statement for healthcare professionals from the American Heart Association. *Circulation* 100:1134–1146, 1999
3. Celentano A, Vaccaro O, Tammaro P, Galderisi M, Crivaro M, Oliviero M, Imperatore G, Palmieri V, Iovino V, Riccardi G: Early abnormalities of cardiac function in non-insulin-dependent diabetes mellitus and impaired glucose tolerance. *Am J Cardiol* 76:1173–1176, 1995
4. Galderisi M, Anderson KM, Wilson PWF, Levy D: Echocardiographic evidence for the existence of a distinct diabetic cardiomyopathy (the Framingham Heart Study). *Am J Cardiol* 68:85–89, 1991
5. Schaffer SW: Cardiomyopathy associated with noninsulin-dependent diabetes. *Mol Cell Biochem* 107:1–20, 1991
6. Factor SM, Borczuk A, Charron MJ, Fein FS, van Hoeven KH, Sonnenblick EH: Myocardial alterations in diabetes and hypertension. *Diabetes Res Clin Pract* 31:S133–S142, 1996
7. Rodrigues B, Cam MC, McNeill JH: Metabolic disturbances in diabetic cardiomyopathy. *Mol Cell Biochem* 180:53–57, 1998
8. Chatham JC, Forder JR, McNeill JH (Eds): *The Heart in Diabetes*. Norwell, MA, Kluwer Academic, 1996
9. Schaffer SW, Mozafferi M: Abnormal mechanical function in diabetes: relation to myocardial calcium handling. *Coron Artery Dis* 7:109–115, 1996
10. Jourdon P, Feuvray D: Calcium and potassium currents in ventricular myocytes isolated from diabetic rats. *J Physiol* 470:411–429, 1993
11. Tsuchida K, Watajma H: Potassium current in ventricular myocytes from genetically diabetic rats. *Am J Physiol* 273:E695–E700, 1997
12. Ren J, Davidoff AJ: Diabetes rapidly induces contractile dysfunctions in isolated ventricular myocytes. *Am J Physiol* 272:H148–H158, 1997
13. Shimoni Y, Firek L, Severson D, Giles W: Short-term diabetes alters K^+ currents in rat ventricular myocytes. *Circ Res* 74:620–628, 1994
14. Ren J, Gintant GA, Miller RE, Davidoff AJ: High extracellular glucose impairs cardiac E-C coupling in a glycosylation-dependent manner. *Am J Physiol* 273:H2876–H2883, 1997
15. Lagadic-Gossmann DL, Buckler KJ, Le Prigent K, Feuvray D: Altered Ca^{2+} handling in ventricular myocytes isolated from diabetic rats. *Am J Physiol* 270:H1529–H1537, 1996
16. Pagliassotti MJ, Prach PA, Koppenhafer TA, Pan DA: Changes in insulin action, triglycerides, and lipid composition during sucrose feeding in rats. *Am J Physiol* 271:R1319–R1326, 1996
17. Podolin DA, Sutherland E, Iwahashi M, Simon FR: A high sucrose diet alters lipid composition and fluidity of liver sinusoidal membranes. *Horm Metab Res* 30:195–199, 1998
18. Podolin DA, Gayles EC, Wei Y, Thresher JS, Pagliassotti MJ: Menhaden oil prevents but not reverses sucrose-induced insulin resistance in rats. *Am J Physiol* 274:R840–R848, 1998
19. Goo AKY, Carson DS, Bjelajac A. Metformin: a new treatment option for non-insulin-dependent diabetes mellitus. *J Fam Pract* 42:612–618, 1996
20. Verma S, Bhanot S, McNeill JH: Antihypertensive effects of metformin in fructose-fed hyperinsulinemic, hypertensive rats. *J Pharmacol Exp Ther* 271:1334–1337, 1994
21. Verma S, McNeill JH: Metformin improves cardiac function in isolated streptozotocin-diabetic rat hearts. *Am J Physiol* 266:H714–H719, 1994
22. Davidoff AJ, Ren J: Low insulin and high glucose induce abnormal relaxation in cultured adult rat ventricular myocytes. *Am J Physiol* 272:H159–H167, 1997
23. Schaffer SW, Ballard-Croft C, Boerth S, Allo SN: Mechanisms underlying depressed Na^+/Ca^{2+} exchanger activity in the diabetic heart. *Cardiovasc Res* 34:129–136, 1997
24. Dhalla NS, Liu X, Panagia V, Takeda N: Subcellular remodeling and heart dysfunction in chronic diabetes. *Cardiovasc Res* 40:239–247, 1998
25. Dai S, McNeill JH: Effects of fructose loading in streptozotocin-diabetic and nondiabetic rats. *Can J Physiol Pharmacol* 70:1583–1589, 1992
26. Misra T, Gilchrist JSC, Russell JC, Pierce GN: Cardiac myofibrillar and sarcoplasmic reticulum function are not depressed in insulin-resistant JCR:LA-cp rats. *Am J Physiol* 45:H1811–H1817, 1999
27. Pierce GN, Russell JC: Regulation of intracellular Ca^{2+} in the heart during diabetes. *Cardiovasc Res* 34:41–47, 1997
28. Feuvray D, Lopaschuk GD: Controversies on the sensitivity of the diabetic heart to ischemic injury: the sensitivity of the diabetic heart to ischemic injury is decreased. *Cardiovasc Res* 34:113–120, 1997
29. Verma S, Bhanot S, McNeill JH: Decreased vascular reactivity in metformin-treated fructose-hypertensive rats. *Metabolism* 45:1053–1055, 1996
30. Ren J, Dominguez J, Sowers JR, Davidoff AJ: Metformin but not glyburide prevents high glucose-induced abnormalities in relaxation and intracellular Ca^{2+} transients in adult rat ventricular myocytes. *Diabetes* 48:2059–2065, 1999

Downloaded from http://diabetesjournals.org/diabetes/article-pdf/50/5/1186/367163/1186.pdf by guest on 06 December 2024